# Anomalous motion of an active deformable particle

Miki Y. Matsuo,* Hirokazu R. Tanimoto, and Masaki Sano
*Department of Physics, The University of Tokyo,*
*Hongo, Bunkyo-ku, Tokyo, Japan*

(Dated: July 5, 2010)

We consider Lévy walk like motion of active deformable particles (ADP) that can move by actively deforming their shape from a circle. A theory is developed by assuming that the equation of velocity includes a coupling with active random deformation. It is shown that the model exhibits a truncated power-law distribution of velocity, whose exponent is determined by the intensity of the random deformation and the strength of the dissipation. In order to apply our model to explain the tracking data of the centroid and the shape dynamics of *Dictyostelium discoideum* cell, we have introduced two variants of ADP model that have the different anisotropies in the deformations.

PACS numbers: 05.40.Fb, 05.70.Ln, 87.17.Jj

The dynamics of self-propelling objects have attracted attention from scientists [1–3]. There have been a number of studies on self-propelled particles, based on both the deterministic dynamics and stochastic dynamics. The motion of a droplet or vesicle under fluctuating circumstances and self-propelling domains in excitable reaction-diffusion media are those of the deterministic self-propelling motions, which were recently investigated [4]. Meanwhile, stochastic self-propelling motions are also investigated with the help of the theory of Brownian motion [5–7]. Although Brownian motion implies a passive equilibrium motion in the naïve sense, the theory of Brownian motion has been applied to various types of active motion. For example, soon after Einstein's theory was published, it was applied to the self-propelling motion of a protozoan [6]. After the progress in computational science, the theory of Brownian motion was used to quantitatively explain the tracking data of living cells [7].

Although many studies of self-propelling motion consider the centroid motion of an object, it was recently noticed how the deformation of a particle affects the centroid. Surprisingly, Ohta-Ohkuma showed that the interaction between the deformation and centroid motion creates a bifurcation sequence from non-moving to straight moving to a circular motion by increasing the velocity of the particle [8]. Their conclusion implies that a coupling between centroid motion and deformation dynamics could provide fruitful variety of dynamics to the particle. Thus, in this paper, we propose a new deformable particle model that provides further fascinating dynamics. We extend the centroid-deformation coupled particle model proposed by Ohta and Ohkuma to create active random deformation, which we call active deformable particle (ADP) in this paper. While investigating the behaviour of ADP, we clarify that it produces fascinating velocity fluctuation; that is, the equilibrium distribution has a functional form that smoothly changes from Maxwellian to Lévy walk like power-law distribution depending on the mutual ratio of intensities of the random centroid motion and random deformation. Finally, we propose applying our ADP model to explain the tracking data of *Dictyostelium discoideum* (Dicty).

First, we provide the fundamental equation of the system analyzed in this paper. We consider a particle in uniform two-dimensional space that can slightly deform from a circular shape to an elliptical shape. Let us denote the centroid velocity of the particle $v_\alpha$ and the deformation tensor $S_{\alpha\beta}$, where $\alpha, \beta = \{x, y\}$. A simple phenomenological description of the dynamics of a deformable particle was provided by Ohta and Ohkuma [9], where the tensor expressing deformation is coupled to the centroid velocity, such that $\dot{v}_\alpha = -\gamma v_\alpha + S_{\alpha\beta} v_\beta + \mathcal{O}(|\boldsymbol{v}|^3)$ by the symmetry argument. Now we modify their model such that the deformation is randomly driven by the internal activeness of the particle. In this case, the velocity $v_\alpha$ and deformation tensor $S_{\alpha\beta}$ are replaced by the stochastic velocity variables $\hat{v}_\alpha$ and $\hat{S}_{\alpha\beta}$

$$\dot{\hat{v}}_\alpha = -\gamma \hat{v}_\alpha + \hat{S}_{\alpha\beta}\hat{v}_\beta + \xi_\alpha, \tag{1}$$

where $\xi$ is centroid noise, $\langle \xi_\alpha(t)\xi_\beta(t')\rangle = 2\sigma_1 \delta_{\alpha\beta}\delta(t-t')$.

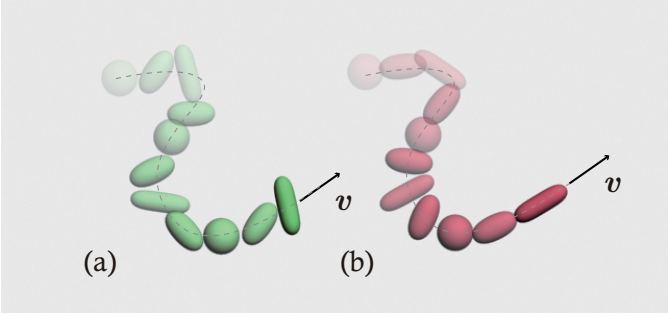


FIG. 1: Two types of active deformable particle. (a) Symmetric ADP. The particle deforms to any direction equivalently. (b) Preferential ADP. The particle prefers to deform to the direction parallel to the velocity $\boldsymbol{v}$.

*Electronic address: miki@daisy.phys.s.u-tokyo.ac.jp

All the calculus in this paper are assumed to be under the Stratonovich definition [10]. Next, we provide an equation for the deformation $\hat{S}_{\alpha\beta}$. Although Ohta-Ohkuma considered the dynamic equation for $S_{\alpha\beta}$, here we assume that $\hat{S}_{\alpha\beta}$ is adiabatically determined by the velocity $\hat{v}_\alpha$ and the noise, assuming that $\hat{S}_{\alpha\beta}$ is sufficiently more rapid than $\hat{v}_\alpha$. A symmetry consideration for the possible interaction between $\hat{v}_\alpha$ and $\hat{S}_{\alpha\beta}$ provides the following two characteristic types of random deformation:

$$\begin{aligned}&\hat{S}_{\alpha\beta} \in \{\hat{S}^{(1)}_{\alpha\beta}, \hat{S}^{(2)}_{\alpha\beta}\},\\ &\hat{S}^{(1)}_{\alpha\beta} \equiv \Xi_{\alpha\beta},\ \hat{S}^{(2)}_{\alpha\beta} \equiv 2\Xi_n(\frac{\hat{v}_\alpha\hat{v}_\beta}{|\hat{\boldsymbol{v}}|^2} - \frac{1}{2}\delta_{\alpha\beta}),\end{aligned} \tag{2}$$

where $\Xi_{\alpha\beta}$ is the symmetric traceless noise tensor as $\Xi_{xx} = -\Xi_{yy}, \Xi_{xy} = \Xi_{yx}$, $\langle\Xi_{xx}(t)\Xi_{xx}(t')\rangle = 2\sigma_{2s}\delta(t-t')$, $\langle\Xi_{xy}(t)\Xi_{xy}(t')\rangle = 2\sigma_{2s}\delta(t-t')$, and $\Xi_n$ is the deformation noise along the direction of velocity satisfying $\langle\Xi_n(t)\Xi_n(t')\rangle = 2\sigma_{2p}\delta(t-t')$. These two types of noisy deformation provide two types of ADP. The $\hat{S}^{(1)}$ provides i) symmetric ADP and the case $\hat{S}^{(2)}$ gives rise to ii) preferential ADP. The symmetric ADP is defined as a particle that deforms to any direction equivalently (Fig.(1), (a)). Meanwhile, the preferential ADP is defined as a particle that has a specific preferential direction of deformation parallel to the centroid velocity (Fig.(1), (b)). Thus, we consider Eqs.(1) and (2) as a fundamental model of ADP. In this paper, we separately analyze these two characteristic ADP, because we can clearly understand each effect in Eq.(2).

First, we consider the first type of ADP, symmetric ADP, where $\hat{S}_{\alpha\beta} = \Xi_{\alpha\beta}$ is assumed. In this case, the stochastic tensor equation (1) can be rewritten in the nonlinear Langevin equation given by

$$\dot{\hat{v}}_\alpha = h_\alpha(\{\hat{v}_\alpha\}) + g_{\alpha\beta}(\{\hat{v}_\alpha\})\eta_\beta, \tag{3}$$

with $\alpha = \{x, y\}$ and $\beta = \{xx, xy, x, y\}$, where

$$h = \begin{pmatrix} -\gamma\hat{v}_x \\ -\gamma\hat{v}_y \end{pmatrix},\ g = \begin{pmatrix} \sqrt{\sigma_{2s}}\hat{v}_x & \sqrt{\sigma_{2s}}\hat{v}_y & \sqrt{\sigma_1} & 0 \\ -\sqrt{\sigma_{2s}}\hat{v}_y & \sqrt{\sigma_{2s}}\hat{v}_x & 0 & \sqrt{\sigma_1} \end{pmatrix}, \tag{4}$$

and $\eta = {}^t(\sigma_{2s}^{-1/2}\Xi_{xx}, \sigma_{2s}^{-1/2}\Xi_{xy}, \sigma_1^{-1/2}\xi_x, \sigma_1^{-1/2}\xi_x)$ Now, in order to translate the Eq.(3) into the corresponding Fokker-Plank equation, we calculate the Kramers-Moyal coefficients $\{D^{(n)}\}$ defined by $D^{(n)}_\alpha(\{v\}, t) \equiv \lim_{\tau\to 0}\langle(\hat{v}_\alpha(t+\tau) - v_\alpha)^n\rangle|_{\hat{v}_\alpha(t)=v_\alpha}/\tau$ [10]. The Fokker-Plank equation is represented with the Kramers-Moyal coefficients as $\partial_t P(\{v\}) = L_{FP}P(\{v\})$ and $L_{FP} = -\partial_{v_i}D^{(1)}_i(\{v\}, t) + \partial_{v_i}\partial_{v_j}D^{(2)}_{ij}(\{v\}, t)$. Using the formulas to calculate the Kramers-Moyal coefficients [10], we get

$$D^{(1)} = \begin{pmatrix} 2\sigma_{2s}v_x - \gamma v_x \\ 2\sigma_{2s}v_y - \gamma v_y \end{pmatrix}, \tag{5}$$

$$D^{(2)} = \begin{pmatrix} \sigma_{2s}(v_x^2 + v_y^2) + \sigma_1 & 0 \\ 0 & \sigma_{2s}(v_x^2 + v_y^2) + \sigma_1 \end{pmatrix}, \tag{6}$$

and the higher order coefficients are all zero. Now, it is useful to rewrite with the polar coordinate, $v_x = v_r\cos\theta$ and $v_y = v_r\sin\theta$. The Fokker-Plank equation represented by the polar coordinate becomes

$$\begin{aligned}\frac{\partial\bar{P}}{\partial t} = \sqrt{\det}\frac{\partial}{\partial v_r}\frac{1}{\sqrt{\det}}\Big((\sigma_{2s}v_r^2 + \sigma_1)\frac{\partial\bar{P}}{\partial v_r}\\ +(\gamma - 2\sigma_{2s})v_r\bar{P}\Big) + \frac{\sigma_{2s}v_r^2 + \sigma_1}{v_r^2}\frac{\partial^2\bar{P}}{\partial\theta^2},\end{aligned} \tag{7}$$

where $\det \equiv (\sigma_{2s}v_r^2 + \sigma_1)^2/v_r^2$ and $\bar{P}$ is a true scaler probability density defined by $\bar{P} \equiv \sqrt{\det}P$ [10]. We are only interested in the equilibrium solution $\bar{P}^*$ whose probability flux is zero. With variable separation $\bar{P}^*(v_r, \theta) = \bar{P}^*_R(v_r)\bar{P}^*_\Theta(\theta)$, $\bar{P}_R$ and $\bar{P}_\Theta$ satisfies

$$(\sigma_{2s}v_r^2 + \sigma_1)\frac{\partial\bar{P}^*_R}{\partial v_r} + (\gamma - 2\sigma_{2s})v_r\bar{P}^*_R = 0,\ \frac{\partial\bar{P}^*_\Theta}{\partial\theta} = 0. \tag{8}$$

These simple differential equations can be exactly solved, and we obtain the general solution written by

$$\bar{P}^*(v_r, \theta) \sim ({v_r}^2 + \sigma_1/\sigma_{2s})^{-\frac{\gamma - 2\sigma_{2s}}{2\sigma_{2s}}}, \tag{9}$$

except for the case $\sigma_{2s} = 0$, where the solution is provided by the Maxwell distribution $\bar{P}^*(v_r, \theta) \sim \exp(-\gamma v_r^2/2\sigma_1)$. This distribution is a truncated power-law distribution with tail $\bar{P}^*(v_r, \theta) \sim {v_r}^{-\frac{\gamma - 2\sigma_{2s}}{\sigma_{2s}}}$ for $v_r \gg \sqrt{\sigma_1/\sigma_{2s}}$. Thus, we attain an impressive relation. The exponent of the power-law tail $P^*(v_r) \sim v_r^{-\mu_s}$ of symmetric ADP is related to the intensity of random deformation as

$$\mu_s = \gamma/\sigma_{2s} - 1, \tag{10}$$

where we used $P \sim \bar{P}v_r^{-1}$ that holds when $v_r \gg \sqrt{\sigma_1/\sigma_{2s}}$. Equation (10) is a kind of fluctuation-dissipation relation (FDR) containing three characteristic quantities $\mu, \gamma$, and $\sigma_{2s}$, which are related to the fluctuation of centroid, dissipation, and the fluctuation of deformation for each.

Now, we consider the second type of deformable particle, preferential ADP. Substituting $\hat{S}_{\alpha\beta} = 2\Xi_n(\hat{v}_\alpha\hat{v}_\beta/|\hat{\boldsymbol{v}}|^2 - \delta_{\alpha\beta}/2)$ into Eq.(1), we get the nonlinear Langevin equation $\dot{\hat{v}}_\alpha = h_\alpha(\{\hat{v}_\alpha\}) + g_{\alpha\beta}(\{\hat{v}_\alpha\})\eta_\beta$ with $\alpha = \{x, y\}$ and $\beta = \{xx, x, y\}$, where $h$ and $g$ are

$$h = \begin{pmatrix} -\gamma\hat{v}_x \\ -\gamma\hat{v}_y \end{pmatrix},\ g = \begin{pmatrix} \sqrt{\sigma_{2p}}v_x & \sqrt{\sigma_1} & 0 \\ \sqrt{\sigma_{2p}}v_y & 0 & \sqrt{\sigma_1} \end{pmatrix}, \tag{11}$$

and $\eta = {}^t(\sigma_{2p}^{-1/2}\Xi_n, \sigma_1^{-1/2}\xi_x, \sigma_1^{-1/2}\xi_x)$. Calculating the Kramers-Moyal coefficients from Eqs.(11), we get

$$D^{(1)} = \begin{pmatrix} \sigma_{2p}v_x - \gamma v_x \\ \sigma_{2p}v_y - \gamma v_y \end{pmatrix}, \tag{12}$$

$$D^{(2)} = \begin{pmatrix} \sigma_{2p}v_x^2 + \sigma_1 & \sigma_{2p}v_xv_y \\ \sigma_{2p}v_xv_y & \sigma_{2p}v_y^2 + \sigma_1 \end{pmatrix}. \tag{13}$$

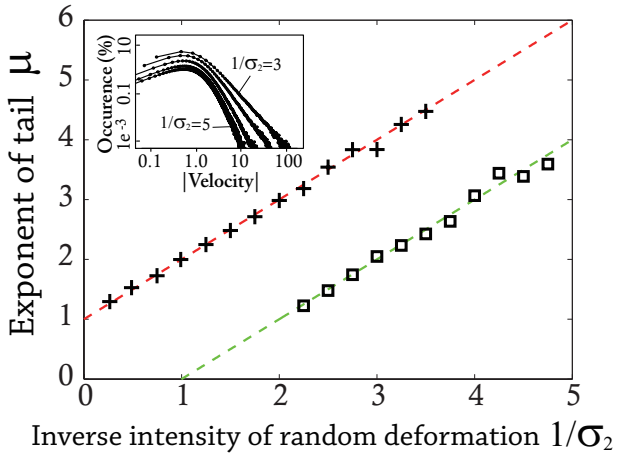


FIG. 2: The relation between exponent of power law tail $\mu$ of velocity distribution and the intensity of random deformation $\sigma_2$. Symbols: numerical simulation; ($\Box$) symmetric ADP, (+) preferential ADP. Dotted line: theoretical prediction; (green) symmetric ADP, (red) preferential ADP. Inset shows the equilibrium velocity distribution $P^*$ of symmetric ADP numerically obtained. The parameters used here are $\gamma = 1, \sigma_1 = 0.01$.

Transforming the coefficient into the polar coordinate, we get the Fokker-Plank equation for preferential ADP

$$\frac{\partial \bar{P}}{\partial t} = \sqrt{\det}\frac{\partial}{\partial v_r}\frac{1}{\sqrt{\det}}\left((\sigma_{2p}v_r^2+\sigma_1)\frac{\partial \bar{P}}{\partial v_r} + (\gamma+\sigma_{2p})v_r\bar{P}\right) + \frac{\sigma_1}{v_r^2}\frac{\partial^2 \bar{P}}{\partial \theta^2}, \qquad (14)$$

where $\det \equiv (\sigma_{2p}v_r^2+\sigma_1)\sigma_1/v_r^2$. Note that the radial part of the Fokker-Plank operator of preferential ADP is almost same to that of symmetric ADP except for the point that the coefficient $\gamma - 2\sigma_{2s}$ in Eq.(7) is now changed to $\gamma+\sigma_{2p}$. Thus we immediately conclude that the equilibrium velocity distribution of preferential ADP becomes

$$\bar{P}^*(v_r,\theta) \sim \left({v_r}^2+\sigma_1/\sigma_{2p}\right)^{-\frac{\gamma+\sigma_{2p}}{2\sigma_{2p}}} \qquad (15)$$

when $\sigma_{2p} \neq 0$, while the distribution becomes Maxwellian when $\sigma_{2p} = 0$. Although the properties of the equilibrium distribution of preferential ADP remain similar, the FDR of preferential ADP is changed from that of symmetric ADP. When $\sigma_{2p} \neq 0$, the equilibrium distribution has a tail as $\bar{P}^*(v_r,\theta) \sim {v_r}^{-\frac{\gamma+\sigma_{2p}}{\sigma_{2p}}}$. Considering the relation $P \sim \bar{P}$ that holds when $v_r \gg \sqrt{\sigma_1/\sigma_{2p}}$, we observe that the exponent of the power law tail $P^*(v_r) \sim {v_r}^{-\mu_p}$ of preferential ADP satisfies

$$\mu_p = \gamma/\sigma_{2p} + 1. \qquad (16)$$

Thus, we have obtained another FDR. The Eq.(10) and (16) are similar in that the exponent of the power-law is proportional to the dissipation divided by the intensity of the random deformation, while they have different non-dimensional constants $\pm 1$ added to the equality. In Fig.(2), we show the numerically obtained FDRs (symbols) solving Eq.(1), where the exponent of tail $\mu$ is calculated by least-square fitting to the numerically obtained equilibrium distribution shown in the inset of Fig.(2). We clearly see that the relation between $\mu$ and inverse $\sigma_{2s,p}$ ($\Box$, + symbols) satisfies Eq.(10) (red line) and Eq.(16) (green line). Thus, the two types of ADP give the different FDRs.

Now, we consider the application of ADP model, especially on biological problems. Most eukaryotic amoeboid cells show centroid movement accompanied with large morphological deformation [11]. The velocity distribution of amoeboid cell has been investigated in detail, and found to be non-Gaussian [12, 13]. Even Lévy walk type search has been considered as the optimal strategy of searching. Recently, Takagi *et al.* suggested that the velocity distribution of Dicty cell has power-law tails [14]. In the previous works, although a heuristic fitting model was used, any mechanism for creating a Lévy walk has not been proposed. Here we can present a possible mechanism for amoeboid cell to create a Lévy walk through the coupling between deformation and centroid motion. It is well-known that intracellular cytoskeleton makes cell membrane deform dynamically [11], and thus, cells can show a Lévy walk as a natural conclusion of our phenomenological theory. Moreover, the ADP models are considered as illustrative models of living cells, because it is known that the shape of an amoeboid cell is highly correlated to the direction of its movement [15, 16].

Thus here, we give a simple estimation to test whether our theory can be applied to an amoeboid cell. A wild-type Dicty cell deforms more and more through its development. Typically, the developmental stage of a Dicty cell is classified into two states, vegetative (VEG, 0 h after the starvation) and starved (STA, several hrs after the starvation) [14]. In these states, the Dicty cell shows distinguishing shapes and motions; the STA cell is more deformed and moves more rapidly than the VEG cell (Fig.(3)(a)). In this paper, we distinguish the following three states of the cell, vegetative, starved 1 (STA1, 2-4 h after the starvation), and starved 2 (STA2, 6-8 h after the starvation), where the STA2 cell is more deformed than the STA1 cell. We can measure the values of three quantities, $\mu, \gamma$, and $\sigma_2$ for each state using imaging analysis. The velocity distributions of these three states have different tails (Fig.(3)(b)), whose values are $\mu_{\rm veg} \simeq 3.6, \mu_{\rm sta1} \simeq 3.7$, and $\mu_{\rm sta2} \simeq 4.2$. We estimate the values of $\gamma$ for VEG, STA1, and STA2 states as $\gamma_{\rm veg} \simeq 0.14, \gamma_{\rm sta1} \simeq 0.090$, and $\gamma_{\rm sta2} \simeq 0.18([\min^{-1}])$ from the decay rate of velocity auto-correlation [17]. The distribution of the scaled length of the cell along the centroid velocity (Fig.(3)(c)) provides the estimation of $\sigma_2$, where the scaled cell length is defined by the cell length divided by mean cell length averaged over the whole observation time and ensemble [17]. Fitting with Gaussian provides $\sigma_{2,\rm veg} \simeq 0.026, \sigma_{2,\rm sta1} \simeq 0.032$, and

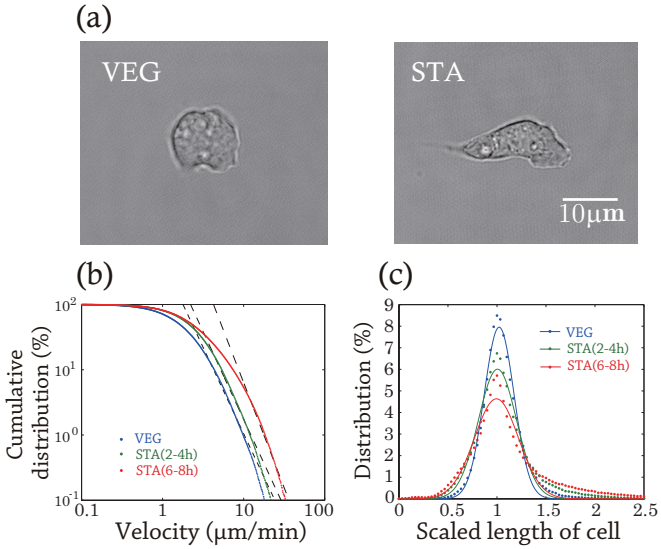


FIG. 3: (a) Typical images of wild-type Dicty cell: (VEG) vegetative state and (STA) starved state. (b) Cumulative velocity distribution of Dicty cells. Fitting the tails of distributions with power law, we get the exponents as $\mu_{\rm veg} \simeq 3.6, \mu_{\rm sta1} \simeq 3.7$, and $\mu_{\rm sta2} \simeq 4.2$ for each state. (c) Distributions of scaled length of Dicty cell along the direction of cell movement (Dot: experiment, Line: fitting). Here the scaled cell length is defined as cell length divided by mean cell length averaged over observation time. Fitting with Gaussian provides $\sigma_{2,\rm veg} \simeq 0.026, \sigma_{2,\rm sta1} \simeq 0.032$, and $\sigma_{2,\rm sta2} \simeq 0.053$. The distributions are calculated from 120 minutes tracks with 1 frame per second of >30 cells.

$\sigma_{2,\rm sta2} \simeq 0.053$. To compare these results with our prediction, we need to know a coefficient which generally exists in the second term of the left-hand-side of Eq.(1), though we eliminated it by an straightforward scaling for the theoretical simplicity. Although we cannot determine this unknown coefficient, we can check whether the FDR is consistent with cell behavior by comparing ratios among observed quantities as $\mu_i \pm 1$ and $\gamma_i/\sigma_i$, where $i$ denotes each state (VEG, STA1, STA2), because the ratio is free from the proportional coefficient. We have degrees of freedom to specify which model (symmetric, preferential) is applied to each state. Among the various scenarios, we observe that the experimental data is roughly explained, when we assume that the VEG cell satisfies the symmetric FDR, and STA1 cell and STA2 cell satisfy the preferential FDR [17]. Thus, we propose that VEG, STA1 and STA2 cells are described with symmetric ADP, preferential ADP, and preferential ADP model, respectively. The change of the effective description is considered due to the development of cell polarity, whose axis is highly correlated to the direction of cell protrusion [11, 18]. We still have several considerable problems. The origin of the nonlinear interaction between the centroid motion and the deformation has to be found from the molecular basis of cell motility. We need much longer data for better estimates of statistical parameters. Without solving these problems, we cannot definitely say that the cell motion obeys the ADP model. However, we consider that our suggestion and estimation are sufficient to promote us to reconsider about the origin of the fluctuation of living cells.

In conclusion, we have analyzed the motion of ADPs, and applied our theory to cell motion. Despite the simplicity and analytical easiness, the ADP model can endow a nontrivial Lévy-type walk to deformable objects with satisfying a simple relation among fluctuation, dissipation and power law behavior. Therefore, we believe our model will be useful as an illustrative model of the anomalous motion of a deformable particle.

We thank T. Ohta, T. Ohkuma, T. Hiraiwa, N. Yoshinaga, H. Chate, and V. Steinberg for fruitful discussions and comments.

[1] T. Vicsek *et al.*, Phys. Rev. Lett. 75, 1226 (1995).
[2] G. Gregoire and H. Chate, Phys. Rev. Lett. 92, 025702 (2004).
[3] F. Peruani and L. G. Morelli, Phys. Rev. Lett. 99, 010602 (2007).
[4] U. Thiele and E. Knobloch, Phys. Rev. Lett. 97, 204501 (2006).
[5] B. Lindner and E. M. Nicola, Phys. Rev. Lett. 101, 190603 (2008).
[6] K. Przibram, Pflgers Arch. Physiol. 153, 401 (1913).
[7] D. Selmeczi *et al.*, Biophysical Journal 89, 912 (2005).
[8] T. Ohta, T. Ohkuma, and K. Shitara, Phys. Rev. E 80, 056203 (2009).
[9] T. Ohta and T. Ohkuma, Phys. Rev. Lett. 102, 154101 (2009).
[10] H. Risken, *The Fokker-Plank Equation* (Springer, Berlin, 1989).
[11] N. Andrew and R. H. Insall, Nature Cell Biol. 9, 193 (2007).
[12] P. J. M. van Haastert and L. Bosgraaf, PLoS ONE 4, e6814 (2009).
[13] L. Li *et al.*, PLoS ONE 3, e2093 (2008).
[14] Takagi *et al.*, PLoS ONE 3, e2648 (2008).
[15] X. Jiang *et al.*, PNAS. 102, 975 (2005).
[16] Y. T. Maeda *et al.*, PLoS ONE 3, 11, e3734 (2008).
[17] See supplementary materials.
[18] L. Bosgraaf, and P. J. M. van Haastert, PLoS ONE 4, e5253 (2009).